INSTITUTE
FOR
AEROSPACE STUDIES

UNIVERSITY OF TORONTO

TP 8101E

FINAL REPORT ON CONTRACT NO. 14SD.T8200-4-4575

AIRSHIP FLIGHT DYNAMICS

Prepared for
Transportation Development Centre

by
Subsonic Aerodynamics Group
University of Toronto Institute for Aerospace Studies

July 1986

CA1
DTC 800
86
A32
c.2

TP 8101E

Library and Information Centre / Centre de Documentation (GSLA)
RECEIVED - REÇU LE
OCT 5 1987
Transport Canada / Transports Canada

FINAL REPORT ON CONTRACT NO. 14SD.T8200-4-4575

AIRSHIP FLIGHT DYNAMICS ANALYSIS

by
Professor J. D. DeLaurier
Justin Amann

Subsonic Aerodynamics Group
University of Toronto Institute for Aerospace Studies

July 1986

The contents of this report reflect the views of the authors and not necessarily the official view or opinions of the Transportation Development Centre of Transport Canada.

Un sommaire en français de ce rapport est inclus avant la Table des Matieres.

Transport Canada / Transports Canada

Development / Développement

REPORT DOCUMENTATION FORM

1. Transport Canada Report No	2. TDC Project No	3. Recipient's Catalogue No.
TP 8101E	6354	

4. Title and Subtitle	5. Report Date
AIRSHIP FLIGHT DYNAMICS ANALYSIS	July 1986
	6. Performing Organization Report No.

7. Author(s)	8. Transport Canada File No.
Justin Amann and Prof. J.D. DeLaurier	D1455-165

9. Performing Organization Name and Address	10. DSS File No.
Subsonic Aerodynamics Group University of Toronto Institute for Aerospace Studies 4925 Dufferin Street Downsview, Ontario M3H 5T6	11. DSS or Transport Canada Contract No. 14SD.T8200-4-4574

12. Sponsoring Agency Name and Address	13. Type of Report and Period Covered
Transportation Development Centre (TDC) 200 Dorchester Blvd. West Suite 601, West Tower Montreal, Quebec H2Z 1X4	14. Sponsoring Agency Code

15. Supplementary Notes	16. TDC Project Officer
	Barry B. Myers

17. Abstract

A six degree of freedom non-linear airship flight simulation program has been developed at the University of Toronto. The program was used to model the flight behaviour of a sample airship, the Airship Industries SKYSHIP 500, for which flight test data was available. The simulation results followed the same general trends indicated by the flight data. The computer simulation performed well in a wide variety of manoeuvres.

18. Key Words	19. Distribution Statement
Nonlinear airship flight simulation	Limited number of copies available from the Transportation Development Centre

20. Security Classification (of this report)	21. Security Classification (of this page)	22. No. of Pages	23. Price
Unclassified	Unclassified	51	

TDC CDT 79.005 Rev 86

Canada

Transports Canada / Transport Canada
Développement / Development

FORMULE DOCUMENTAIRE DU RAPPORT

1. N° du rapport Transports Canada	2. N° de l'étude — CDT	3. N° de catalogue du destinataire
TP8101E	6354	

4. Titre et sous-titre	5. Date du rapport
AIRSHIP FLIGHT DYNAMICS ANALYSIS	Juillet 1986
	6. N° du rapport de l'organisme exécutant

7. Auteur(s)	8. N° de dossier Transports Canada
Justin Amann et Prof. J.D. DeLaurier	D1455-165

9. Nom et adresse de l'organisme exécutant	10. N° de dossier — ASC
Subsonic Aerodynamics Group University of Toronto Institute for Aerospace Studies 4925 Dufferin Street Downview, Ontario M3H 5T6	11. N° de contrat — ASC ou Transports Canada 14SD.T8200-4-4574

12. Nom et adresse de l'organisme parrain	13. Genre de rapport et période visée
Centre de développement des transports (CDT) 200 ouest, boul. Dorchester Suite 601, Tour ouest Montréal (Québec) H2Z 1X4	14. Code de l'organisme parrain

15. Remarques additionnelles	16. Agent de projet — CDT
	Barry B. Myers

17. Résumé

Le programme non linéaire à six degrés de liberté étudié et mis au point par l'Université de Toronto a été utilisé pour simuler le vol d'un aérodyne, en l'occurrence un dirigeable SKYSHIP 500 fabriqué par Airship Industries, pour lequel on disposait déjà de l'information tirée des essais de vol auxquels il avait été soumis. Les résultats fournis par la simulation ont été analogues aux résultats des essais de vol, vérifiant ainsi la bonne performance du modèle informatique dans toute l'étendue du domaine considéré.

18. Mots-clés	19. Diffusion
Programme de simulation non linéaire pour aérodyne	Le Centre de développement des transports dispose d'un nombre limité d'exemplaires

20. Classification de sécurité (de ce rapport)	21. Classification de sécurité (de cette page)	22. Nombre de pages	23. Prix
Non classifié	Non classifiée	51	

SUMMARY

This report discusses a six degree of freedom nonlinear airship flight simulation program which has been developed at the University of Toronto. The program was tested using the Airship Industries SKYSHIP 500 as a sample airship. SKYSHIP 500 flight test data were available for a wide variety of manoeuvres. The simulation program was run for the same set of manoeuvres to see how closely predictions would match measured results.

The simulation is essentially a means of solving the vehicle's equations of motion. At a given instant in time the airship has a certain orientation and velocity. These give rise to aerodynamic, gravity, buoyancy and inertial forces and moments which act on the blimp. Solving Newton's second law (F=ma) gives the accelerations, which are integrated over time to give velocities and orientations at the next time increment. By repeating this over and over a flight is simulated.

The airship is modelled as a rigid body. The hull is divided lengthwise into segments for the purpose of calculating aerodynamic loads. Aerodynamics are dominated by the hull and fins, and aerodynamic forces on the gondola are neglected.

Information about the SKYSHIP 500 that was known prior to the project consisted of a three-view drawing, maximum take-off weight and cruise speed. Weight breakdown and aerodynamic properties necessary for the simulation were estimated from this information.

The simulation was used to put the SKYSHIP 500 through a series of

manoeuvres. These tests measured trim drag, turn rate versus rudder angle, frequency response to control inputs and transient response to throttle inputs. The simulation predicts drag well in straight trimmed flight but underpredicts drag by 10-25% in steady turning flight. Accuracy is better for the higher yaw rates. The same runs show that the simulation underpredicts yaw rate for a given rudder angle at 25 knots, but agrees with measured results at 40 knots.

Frequency response tests were simulated by giving the elevator or rudder a frequency sweep. A Fast Fourier analysis was performed on the results to obtain gain and phase relationships between output and input. Predicted frequency response of pitch rate to elevator angle agreed with measured response at low frequencies but was too low at higher frequencies. Phase angle prediction was excellent. Predicted roll response to rudder input was very good. The roll pendulum mode was clearly identified, although it attenuated too quickly above 1 rad/s. Predicted yaw response was excellent, as were phase angles for both roll and yaw.

To examine transient response to throttle inputs the blimp was first set hovering. Then throttles were stepped up and after an interval were returned to zero. Three tests were performed, with engines set to give forward thrust, vertical thrust and differential thrust. Predicted velocities, accelerations and rotation rates agreed very well with flight test results.

Overall the computer simulation predictions matched flight test results of the SKYSHIP 500 very well.

Sommaire

Ce rapport traite du programme non linéaire à six degrés de liberté utilisé pour simuler le vol d'un aérodyne. Étudié et mis au point par l'Université de Toronto, ce programme a été vérifié par confrontation de ses résultats avec ceux des essais de vol du dirigeable SKYSHIP 500 fabriqué par Airship Industries. Dans ce but, les manoeuvres simulées ont émulés celles auxquelles le dirigeable avait été déjà soumis.

La simulation est une méthode permettant de résoudre les équations du mouvement d'un mobile, en l'occurrence le dirigeable. En effet, à chaque instant celui-ci possède une orientation et une vitesse données, correspondant aux forces et aux moments agissant sur lui: forces aérodynamiques, pesanteur, force ascensionnelle et inertie. La deuxième loi de Newton (F=ma) donne les accélérations dont on réalise les intégrations dans le temps pour obtenir l'orientation et la vitesse du dirigeable à l'instant incrémentiel suivant, et ainsi de suite de manière à simuler la dynamique d'un vol.

Le modèle informatique considère le dirigeable comme un corps rigide subdivisé en segments perpendiculaires à l'axe longitudinal pour les fins du calcul des forces aérodynamiques. Le comportement aérodynamique d'un dirigeable est dicté surtout par les charactéristiques de sa coque et de ses gouvernes, les forces agissant sur la nacelle sont considérées comme négligeables.

Au sujet du SKYSHIP 500, les caractéristiques connues au moment du lancement du projet étaient la masse maximale au décollage et la vitesse de croisière; on disposait en outre d'un plan trois vues du dirigeable. À partir

de ces informations, la masse de chacun des éléments ainsi que leurs caractéristiques aérodynamiques ont été déterminées par calcul et utilisées dans le modèle de simulation.

Par la simulation, le dirigeable a été soumis à une série de manoeuvres destinées à mesurer la traînée d'équilibrage, la vitesse angulaire de virage en fonction de l'angle de braquage du gouvernail de direction, la réponse en fréquence en réaction aux commandes et la réponse dynamique aux variations de poussée. En vol rectiligne uniforme, les résultats théoriques de traînée sont proches des résultats mesurés, mais en virage stabilisé, ceux-là sont inférieurs à ceux-ci de 10 à 25 p. 100. La justesse de la simulation s'améliore aux valeurs élevées de vitesse angulaire de lacet. De même, à la vitesse de 25 noeuds et pour un angle de braquage donné, les résultats théoriques tombent en deça de la réalité pour ce qui est de la vitesse angulaire de lacet, mais il y a concordance à la vitesse de 40 noeuds.

Les essais de réponse en fréquence ont été simulés en soumettant tour à tour les gouvernes de direction et de profondeur à des variations de fréquences. Les résultats ont été traités par transformation de Fourier rapide pour en extraire les relations de gain et de phase entre les valeurs d'entrée et celles de sortie. Les variations en tangage en réaction aux variations des angles de braquage de la gouverne de profondeur se sont révélées, en simulation, identiques aux valeurs mesurées lorsque les fréquences sont basses, et trop basses lorsque les fréquences sont élevées. La concordance des valeurs de phase a été excellente et la concordance très bonne dans le cas de la réponse en roulis aux variations de la gouverne de

direction. La réponse en roulis de mode pendulaire a été bien mise en évidence, bien que la simulation montre un amortissement trop rapide du roulis aux valeurs supérieures à 1 radian/s. Pour ce qui est de la réponse en lacet, la concordance a été excellente, ainsi que pour les valeurs de phase tant en roulis qu'en lacet.

En vue de déterminer la réponse dynamique du dirigeable aux variations de poussée, on a commencé par mettre celui-ci en état de vol stationnaire. Ensuite, les manettes des gaz ont été poussées et maintenues dans cette position pendant un certain temps. Enfin, elles ont été ramenées à la poussées zéro. Trois essais ont été faits, les moteurs ayant été réglés pour donner une accélération respectivement vers l'avant, le haut et différentielle. La concordance a été très bonne pour les trois paramètres de vitesse, d'accélération et de vitesse angulaire.

Tout compte fait, la concordance des résultats théoriques et des résultats mesurés a été très bonne.

TABLE OF CONTENTS

	Page
1. INTRODUCTION	1
2. DESCRIPTION OF THE FLIGHT SIMULATION	2
3. ANALYTICAL MODEL OF THE AIRSHIP	3
3.1 Physical Assumptions	3
3.2 Aerodynamic Assumptions	4
4. DESCRIPTION OF THE DATA BASE	5
5. COMPARISON WITH FLIGHT TEST RESULTS	8
5.1 Trim Required vs Trim Airspeed	8
5.1.1 Method of Trimming	8
5.1.2 Straight line Thrust	9
5.1.3 Trim Thrust in Turns	10
5.2 Yaw Rate vs Rudder Deflection	11
5.3 Frequency Response to Pitch Yoke	12
5.4 Frequency Response to Yaw Yoke	13
5.5 Transient Response to Throttle Step and Return	13
6. RECOMMENDATIONS	16
7. CONCLUSIONS	17
8. REFERENCES	18
FIGURES	19-28
TABLES	29-34
APPENDIX I - System Equations of Motion	35-37

LIST OF FIGURES AND TABLES

Figures — Page

Fig 1 - Hull Coordinate System and Sectioning Scheme 19
Fig 2 - Thrust Required vs Trim Airspeed in Steady Turns 20
Fig 3 - Transient Response to Rudder Step 21
Fig 4 - Steady Yaw Rate vs Rudder Deflection 22
Fig 5 - Frequency Response of Pitch Rate to Elevator Input at 40 knots 23
Fig 6 - Predicted Response of Skyship 500 to Rudder Sweep at 40 knots 24
Fig 7 - Frequency Response of Roll Rate to Rudder Input 25
Fig 8 - Frequency Response of Yaw Rate to Rudder Input 25
Fig 9 - Response to Throttle Step and Return From Hover - Forward Thrust 26
Fig 10 - Response to Throttle Step and Return From Hover - Upward Thrust 27
Fig 11 - Response to Throttle Step and Return From Hover - Differential Thrust 28

Tables

Table 1 - Summary of Basic SKYSHIP 500 Properties 29
Table 2 - Summary of Estimated SKYSHIP 500 Properties 30
Table 3 - Hull Physical Properties (Ballonet Volume = 12% Hull Volume) 31
Table 4 - List of Aerodynamic Parameters 34

NOMENCLATURE

A_{ij} system inertia matrix

a_2 rate of change of fin lift coefficient with control angle

$(C_{dc})_f$ fin cross-flow drag coefficient, referenced to area S_f

$(C_{dc})_h$ hull cross-flow drag coefficient, referenced to area J_1

$(C_{df})_0$ fin zero-angle axial drag coefficient, for only one side of the fin, referenced to area S_f

$(C_{dh})_0$ hull zero-angle axial drag coefficient, referenced to wetted area

$(C_{n\alpha})_f$ derivative of the isolated fin's normal force coefficient with respect to α, at $\alpha=0$ and referenced to S_f

CL, CD lift and drag coefficients, referenced to S_h

CM pitching moment coefficient about nose, referenced to S_h and ℓ

c.g. centre of gravity

c.v. centre of volume

c mean aerodynamic chord of a fin panel

HXY gain of transfer function (output/input)

I_{xx}, I_{yy}, I_{zz}, I_{xz} moments of inertia

J1 hull integral, $J1 = \int_0^h 2r\,dx$

k_1 axial apparent mass coefficient of the hull

k_2, k_3 transverse apparent mass coefficients of the hull

ℓ total hull length

$(\ell)_1$ distance from nose of hull to aerodynamic centre of a fin

$(\ell)_2$ distance from nose of hull to centre of mass of a fin

ℓ_h distance between the nose and the intersection point of the fin's leading edge with the hull

m airship mass

M_{a1} axial apparent mass of the hull

M_{a2}, M_{a3} transverse apparent masses of the hull

S_{fe} planform area of exposed portion of a single fin

S_f planform area of a single fin

P,Q,R angular velocity components in c.v. frame

PHI,THETA,PSI Euler roll, pitch and yaw angles

U,V,W velocity components in c.v. frame

x, y, z coordinates in nose-fixed frame of reference, see Figure 1

X_{cg}, Y_{cg}, Z_{cg} position of c.g. relative to c.v.

α angle of attack, angle between hull centreline and incoming wind

α' modified angle of attack for fins with anhedral

η_f fin-efficiency factor accounting for the effect of the hull on the fins

η_k hull-efficiency factor accounting for the effect of the fins on the hull

η_t leading edge suction efficiency factor (η_t=0 for sharp leading edges and η_t=1 for perfect leading edge suction)

ξ axial integration variable

ξ_{cvi} axial integration variable with respect to centre of volume of i^{th} hull section

δ_e elevator deflection

δ_r rudder deflection

1. INTRODUCTION

The purpose of this report is to present the findings of a comparison between a computerized flight simulation and actual flight test data for the Airship Industries SKYSHIP 500 airship. The intent of this project is to determine the accuracy of the computer simulation in predicting ...hip flight behaviour.

The computer flight simulation was developed at the University of Toronto Institute for Aerospace Studies by Prof. J. D. DeLaurier and his research group. It has been adapted for specific application to the SKYSHIP 500. Properties of this airship were extracted from or derived from drawings and charts in a PACE report (Ref 1) regarding the SKYSHIP 500's performance as a maritime patrol vehicle.

The Patrol Airship Concept Evaluation (PACE) report provides qualitative and quantitative data regarding the SKYSHIP 500's performance in various manoeuvres. The goal of this project is to duplicate any manoeuvres for which quantitative results were available using the airship flight simulation program and see how the results compare with the actual flight test data.

2. DESCRIPTION OF THE FLIGHT SIMULATION

The six degree-of-freedom non-linear flight simulation used in this project is essentially a means of solving the airship's equations of motion. The flight simulation is termed "non-linear" because the forces and moments are non-linear functions of vehicle orientation and velocity (i.e. no small angle approximations have been made).

The principle behind the simulation is simple. The airship is placed in an inertial frame with an initial orientation and velocity. The orientation and velocity allow the program to calculate the relative wind components in a body-fixed stability-axes frame. Aerodynamic, buoyant, gravity and thrust forces are calculated in this frame. Accelerations of the six degrees of freedom are solved for using Newton's second law. These accelerations are then integrated over a time Δt by a Runge-Kutta method to find the velocity and orientation at the new instant in time. This process is repeated over and over to produce a simulated flight. Note that the force analysis is done in the body-fixed frame, while vehicle orientation is described in a ground-fixed frame.

The program contains subroutines that calculate the aerodynamic forces and moments on each hull and fin panel, a routine to trim the blimp, and an autopilot routine that provides thrust and control commands. The workings of the simulation are explained more thoroughly in references 2 and 3.

Note that this simulation program is also capable of calculating shear force and bending moment distribution along the length of the vehicle in flight. It can calculate these loads during manoeuvres and during gusts.

3. ANALYTICAL MODEL OF THE AIRSHIP

3.1 Physical Assumptions

The airship is assumed to be a rigid body. It is assumed to be axisymmetric, except that the horizontal fins may have some anhedral. Air is contained in fore and aft spheres inside the hull; this models the SKYSHIP 500's ballonets. The ballonets are fixed and are not free to move around inside the hull envelope. The remainder of the hull envelope contains helium. Fins, nosecone and gondola are rigidly attached to the body. The dynamic flight equations are taken with respect to the hull centre of volume. These equations are shown in Appendix I (from Ref 3).

The body is assumed to be a body of revolution, consisting of a shell with weight equal to that of the hull envelope and internal catenary cable structure. The gondola,payload and engines are assumed to be a point mass located at the gondola's mass centre. The airship mass centre lies directly below the hull centre of volume when the airship is neutrally buoyant or hovering. The mass centre is shifted forward to maintain trim in forward flight. This is done on the actual SKYSHIP 500 by pumping air from the rear ballonet to the forward ballonet.

The fins are assumed to be point masses located at the mass centres of the fins. Vectored thrust is modelled by giving each engine its own thrust setting and its own angle from the horizontal.

A more detailed description of the airship model is given in Appendix D of reference 2. Note that any differences in the air/gas model have already been discussed above.

3.2 Aerodynamic Assumptions

It is assumed that the aerodynamic properties of the airship are dominated by the hull and the fins, and that the aerodynamic forces on the gondola can be ignored.

The SKYSHIP 500 was divided into 9 segments, seven ahead of the fins, one containing the fins and one behind. The aerodynamics in the region ahead of the hull-fin intersection are dominated by the hull, but modified by the fins using an experimentally derived efficiency factor. The aerodynamics in the fin region are dominated by the fins but modified by the body using another efficiency factor. Fig 1 shows the hull sectioning scheme as well as the coordinate system by which the hull geometry is defined.

4. DESCRIPTION OF THE DATA BASE

The data regarding the SKYSHIP 500 that was known prior to this project is listed in Table 1. This data was found in drawings and tables found in the PACE report. One change was made in this table since the progress report (Ref 4) was written : maximum cruise speed was reduced from 62 kn to 55 kn.

Additional data that was necessary to begin this project appears in Table 2. This data was all estimated. At the time of the first progress report, the estimated data was obtained by comparison with a similar sized airship, the Grace Airship Corporation GAC-20-138 airship (ref 5). Since that time changes have been made to the estimates of several component weights. These changes reflect the advanced technology used in the SKYSHIP 500 construction compared to that of the Grace airship.

Specific changes in estimates are as follows. All fins will be assumed to have the same weight, 273 lb (124.2 kg). The nose is comprised of two parts, the nosecone and battens, weighing 242 lb, and the nose ballast, which weighs 165 lb. The gondola weight has been increased slightly from 3757 lb to 3865 lb. Envelope weight has been increased from 2096 lb to 2638 lb. Manufacturer's empty weight was increased from 224.92 slugs to 248.62 slugs. This new empty weight was obtained by summing new estimated weights of the airship components.

The airship is divided axially into a number of segments, so as to allow precise modelling of the aerodynamic and inertial loads on the vehicle. The first seven segments lie in the "hull region" ahead of the hull-fin intersection. The region containing the fins is known as the "fin

region". The ninth section lies aft of the fin region. The sectioning scheme appears in Figure 1 along with the coordinate axes used to define the airship geometry.

Another change in the data base involves the method of modelling the air and helium distribution in the envelope. Previously the air was assumed to lie in a uniform layer on the bottom of the envelope with the helium occupying the volume above the air. The new method models the SKYSHIP 500's dual ballonet system more accurately. The ballonets are represented as spheres sitting on the bottom of the hull. One ballonet is mounted foreward in the hull such that half of it is in hull section 2 and half in hull section 3. The aft ballonet is shared by hull sections 7 and 8. This model allows more accurate mass property estimation. It also gives the simulation program the capability to trim the airship by pumping air between ballonets, as is actually done on the SKYSHIP 500. The mass properties that appear in this report are for a nominal flight condition where both ballonets contain the same amount of air.

Hull sectioning was performed as in the progress report. (See Table 3 of that report). Hull geometric properties have not changed, and appear in Table 4 of that report.

Table 3 of this report contains the revised hull physical properties of each section when the ballonets are 12% full. The airship has a total mass of 420 slugs (including gases) and is neutrally buoyant in the nominal flight case. Note that the SKYSHIP 500 can fly with a slight "static heaviness" by using an angle of attack to give extra lift.

Changes have also been made to many of the aerodynamic parameters listed in Table 8 of the progress report. A new list appears in Table 4 of this report. The changes were simple re-referencing of

coefficients to agree with the reference surface areas in the simulation program.

5. COMPARISON WITH FLIGHT TEST RESULTS

The PACE report gives quantitative and qualitative results for various flight test manoeuvres of the SKYSHIP 500. The goal of this project was to apply the simulation program to those flight tests for which quantitative results were obtained. These tests include :

i) thrust required vs trim airspeed

ii) steady yaw rate vs rudder deflection

iii) frequency response to pitch yoke at 40 knots

iv) frequency response to yaw yoke at 40 knots

v) transient response to throttle step and return (duct angle at 0 deg, 90 deg and differential thrust)

The subsections that follow present the results of the computer flight simulation along with the PACE results. Each subsection begins with a brief discussion of the autopilot actions and finishes with a discussion of the computer simulation results for that manoeuvre.

5.1 Thrust Required vs Trim Airspeed

5.1.1 Method of Trimming

There are four variables that are used to trim the SKYSHIP 500 for straight horizontal flight at a given airspeed. They are thrust, pitch angle θ, elevator angle β and centre of mass location Xcg.

When the blimp is neutrally buoyant, the easiest way to trim is to set pitch angle and elevator angle to zero. Thrust is then set to overcome zero-angle drag and c.g. location is set so that the weight moment

overcomes the thrust moment about the centre of volume.

When the blimp is statically heavy, the airship must be flown at a positive angle of attack to produce the lift for level flight. The throttles are set to maintain constant airspeed, ballonets are adjusted to move the c.g. and give slight positive pitch and the elevator is slightly trailing edge down for lift. It should be noted that most of the trimming capability is provided by the ballonets and that the elevators are used mainly for control during flight. Also, all of the simulated flights were performed with the airship neutrally buoyant.

Once trim is achieved, thrust, ÷ℋℰ÷A and β are set, and the autopilot does not perform any control function for straight flight. For turning flight the autopilot initiates the turn using a rudder deflection at a specified time. Once the airship is settled into a steady turn, the velocity and yaw rate produced by the trim thrust (for a given rudder angle) are recorded.

5.1.2 Straight Flight Thrust

The straight line required thrust as predicted by the computer simulation falls almost exactly on the curve from the PACE report, as shown in Fig 2. Original estimates for $(C_{dh})_o$ and $(C_{df})_o$ underpredicted drag, and were adjusted to provide the same drag as was experimentally obtained in the PACE project. A drag area of 100 ft^2 results. Based on frontal reference area, C_{df}=0.60, which is typical for large streamline bodies with turbulent boundary layers. Based on wetted surface area of the entire hull this gives C_{dw}=0.0056.

5.1.3 Trim Thrust in Turns

Thrust required in steady turns increases sharply, due to the relatively large sideslip angles (typically 8-12 degrees) and resulting higher induced drag required to turn the airship. High sideslip angles are needed since the aft rudders produce lift opposite to the required turning force. Fig 2 shows thrust levels required to achieve various yaw rates as a function of airspeed.

The results compare well between the computer simulation and PACE. Both show the same trends. As seen on Fig 2 the computer simulation underestimates drag by 10-25% at low yaw rates but is more accurate at higher yaw rates.

The simulation predicts trim thrust quite well. In straight flight the calculated thrust matches measured thrust almost exactly. In steady turns it underpredicts total drag by about 10-15% at low yaw rates but is very accurate at high yaw rates.

Note that several aerodynamic parameters (inputs to the simulation program) were adjusted to make the simulation results correspond so closely to experimental results. In particular, $(C_{dc})_h$ was brought down to 0.2. In order to get good results from the dynamic simulation, good input data is a must. Present methods of theoretically predicting aerodynamic parameters such as $(C_{dc})_h$ are not yet fully developed, and until good wind tunnel data becomes available the simulation can only be validated by making adjustments to the input data where it is reasonable to do so.

5.2 Yaw Rate vs Rudder Deflection

At a given airspeed, turn rate is a function of rudder angle. Steady turns were initiated as discussed in section 5.1. Fig. 3 shows plots of rudder deflection, forward velocity (u), sideslip velocity (v), roll angle (ΠΗι), yaw rate (R) and heading angle (PSI) as functions of time. These show the transient response of the airship to rudder input as the airship goes into a steady turn. Note that in an actual flight the pilot would increase thrust to maintain airspeed in the turn, but that the computer program does not presently have that capability.

Fig 4 shows the results of this flight test from both the simulation and the PACE report. At 25 knots the PACE flight test curve showed a slight non-linearity between rudder angle and yaw rate, which was amplified by the simulation. The simulation underpredicts yaw rate R at 25 knots by up to 30%. At 40 knots the PACE curve was linear, and predicted values agree with the flight test curve.

Also, as noted in fig 4, the PACE report revealed a region of unsteadiness in R and δ_r for low rudder angles. This unsteadiness is due to a slight directional instability (typical for an airship) at low sideslip angles. The PACE report explains that during straight flight there is a continuous hunting of the yaw rate and turn control, and that a residual turn rate of below 1-2 deg/sec at zero rudder deflection had to be cancelled by continuous rudder activity. This effect was not uncovered by the simulation.

When sideslip is large enough to cause a yaw rate of about 1-2

deg/s (i.e. rudder angle above 4 deg) there was no scattering of the points, and the airship held a steady turn. This positive directional stability at larger sideslip angles agrees with the PACE results.

The computer simulation predicts steady turn yaw rate vs rudder angle to be very close to that measured in the PACE flight tests.

5.3 Frequency Response To Pitch Yoke

For the PACE program frequency sweeps were performed on the SKYSHIP 500 at 25 and 40 knots. Frequency sweeps provide an efficient measure of the describing function between a given control and several simultaneously recorded variables. From these sweeps BODE plots and other transfer function data can be calculated, if fast-Fourier transform techniques are available. STI (one of the supporting agencies in the PACE project) was able to analyse all data using its proprietary fast-Fourier transform computer program. This program enabled them to compute gain and phase relationships and many other parameters at each input frequency, and also develop Bode plots. The luxury of such an analysis program was recently made available for the project at hand.

For this test the airship was initially in trimmed flight at 40 kn. The pilot then started an elevator frequency sweep, oscillating the pitch yoke at a low frequency and continuously increasing the frequency. Frequency response of pitch rate to elevator angle was analyzed and is presented in fig.5. At the left are elevator and pitch rate time series which were generated by the simulation. To the right are the Bode plots for Q/δ_e. Magnitude and phase angle of the transfer function are

presented. Experimental data are plotted with the simulation predictions for comparison. Predicted Q response is about 5 dB too low over most of the frequency range (0.1 - 5.0 rad/s). Phase angle prediction matches very closely.

5.4 Frequency Response to Yaw Yoke

In this test the rudder is given a frequency sweep much like the elevator was in the previous test. Fig.6 shows the response of all relevant degrees of freedom for a rudder frequency sweep at 40 kn. Fig.7 and 8 show Bode plots for roll and yaw response to rudder. Predicted roll response agrees well with experimental results. Agreement is excellent up to 0.8 rad/s. The simulation distinguishes the roll peak at 1.1 rad/s, although the predicted peak is about 5 dB too low. Also, above 3 rad/s estimated P attenuates more sharply than experimental P. Predicted yaw response is in excellent agreement with measured response. Phase angle prediction is also excellent for both roll and yaw.

5.5 Transient Response to Throttle Step and Return

These tests show transient response of the airship to throttle inputs. Starting from hover, the blimp was given step throttle inputs of three types:

i) forward thrust (engine duct angle = 0^0)

ii) upward thrust (engine duct angle = 90^0)

iii) differential thrust (one engine duct at 0^0, the other at 180^0).

The response of the airship to each of these inputs is discussed below. Note that the upward and differential thrust cases involve high angle crossflow over the hull and fin panels.

Forward Thrust

For the forward throttle test, fig.9a and b show the experimental and predicted results for all relevant variables. Thrust is 540 lb/engine applied over the interval 6<t<34 seconds. Note that the prediction plots in fig.9b are plotted on different scales than the experimental results of fig.9a, such that the shapes of the curves are the same but magnitudes look different at first. Plots of the same variables are presented side by side where possible. Fig.9a shows that forward velocity U (PACE calls this V) goes up to 35 kn @ 40 mph. The simulation predicts 40 mph. Both show that Q pulses up to 2.5 deg/s. Axial acceleration curves have the same shape for both experiment and computer. Acceleration magnitudes vary because the simulation gives accelerations at the hull c.v., while in the flight tests accelerometers were displaced from the airship c.v.. Included in the simulation variables are pitch angle and altitude. As expected, the thrust moment caused the airship to pitch up and climb.

Upward Throttle

For the upward throttle test the thrust level was set at 360 lb/engine. The thrust is applied over the interval 8<t<39 seconds. Fig.10a and b show relevant variables from flight tests and simulation. Predicted response of Q, A_X, A_Z and U agree almost exactly in shape with

flight test results. Predicted climb rate is about 400 ft/min, which agrees with experiment.

Differential Throttle

For this pirouette manoeuvre, thrust was set at 150 lb/engine. Thrust was applied for the period 24<t<55 seconds. Fig 11a and b show the response of relevant variables. A maximum yaw rate of -6 deg/s appears in both sets of data. A very small roll oscillation appeared at 1.1 rad/s in both simulation and experiment. This corresponds to the airship's roll pendulum mode. The simulation modelled the airship as a rigid body, and it was therefore impossible to capture the 1.2 Hz cab-on-hull structural mode (cab dangle mode) that the experiment revealed.

The simulation program was able to match all the major trends that appeared in the flight test data. In most instances prediction matched experimental results very closely, and verified the program's ability to model transient responses and high angle crossflows.

6. RECOMMENDATIONS

Future work might include a computer program to help estimate aerodynamic parameters. A method of backtracking from flight test data to find force, moment and efficiency coefficients would aid in the development of future parameter estimation techniques.

7. CONCLUSIONS

The six-degree-of-freedom non-linear airship flight simulation program is an effective tool for analysing the behaviour of airships. It can be used to calculate drag in manoeuvres, as well as giving a time history of all degrees of freedom in response to any control inputs.

8. REFERENCES

1. Bailey, David B., "Patrol Airship Concept Evaluation (PACE)", Naval Air Development Center, Airtask No. 62241N/F41-411/DH814, March 1985.
2. DeLaurier, J. D., Evans, J. R., Scholaert, H., "A Study of Airship 6-Degree-of-Freedom Non-Linear Flight Dynamics", University of Toronto-York University Joint Program in Transportation, Research Report No. 79, July 1981.
3. Lowe, J. D., "Heavy Lift Airship Dynamics", M.A.Sc. Thesis, University of Toronto, Institute for Aerospace Studies, 1984..
4. Amann, Justin, "Airship Flight Dynamic Analysis", Progress Report to Transportation Development Centre, Jan. 1986.
5. Lowe, J. D., "Physical and Aerodynamic Properties of the Grace Aircraft Corporation GAC-20-138 Airship", Contrator Report for J. D. DeLaurier & Associates, Nov. 1985.

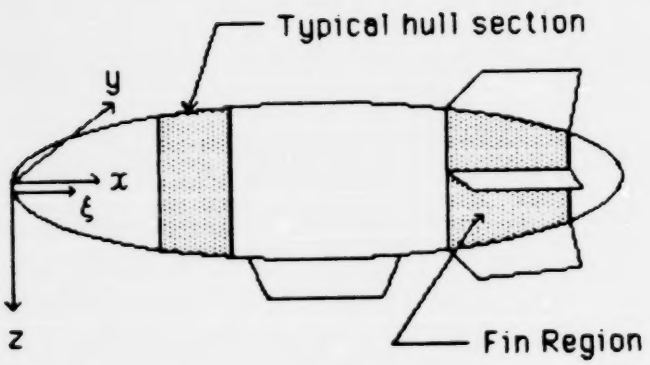

Fig 1 - Hull Coordinate System and Sectioning Scheme

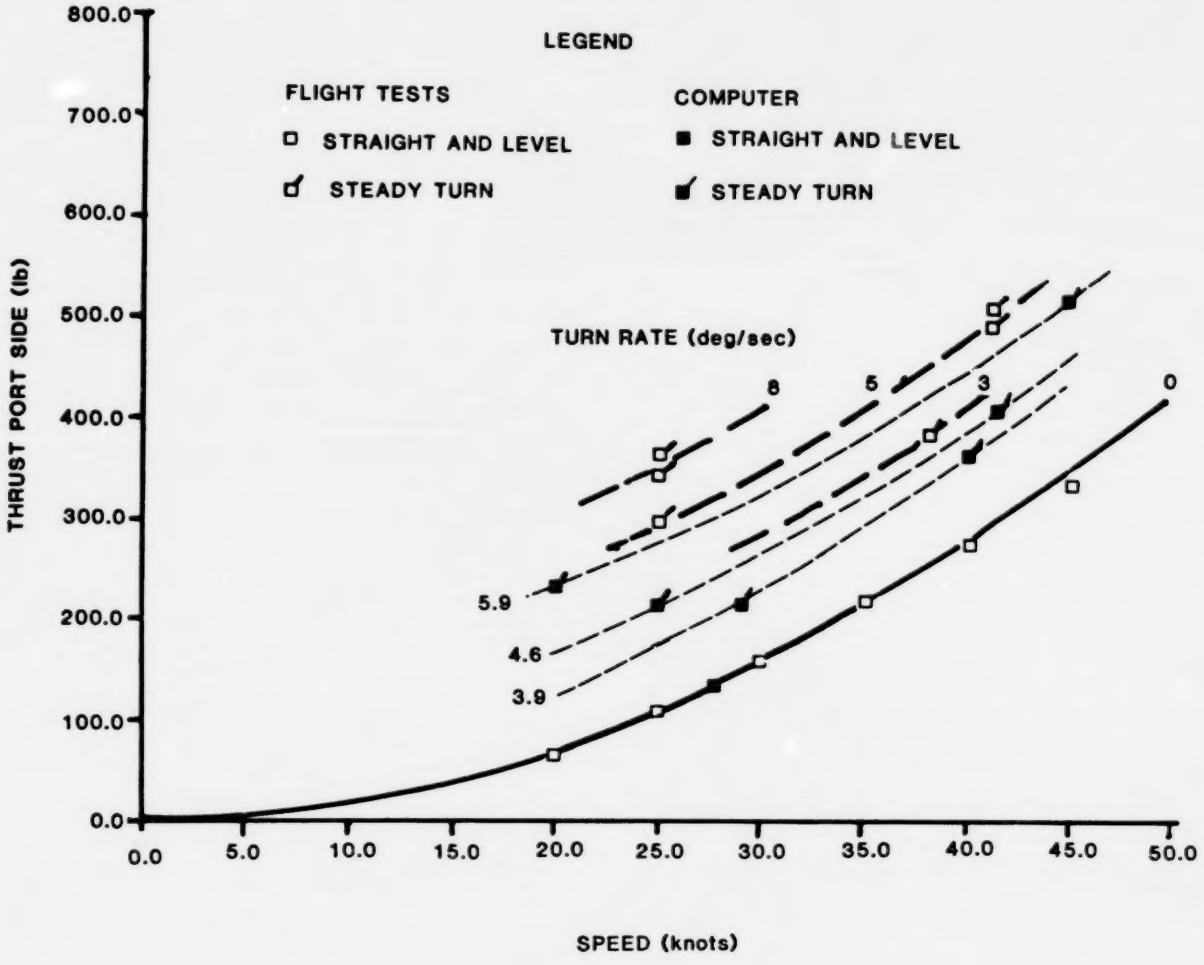

Fig 2 - Thrust Required vs Trim Airspeed in Steady Turns

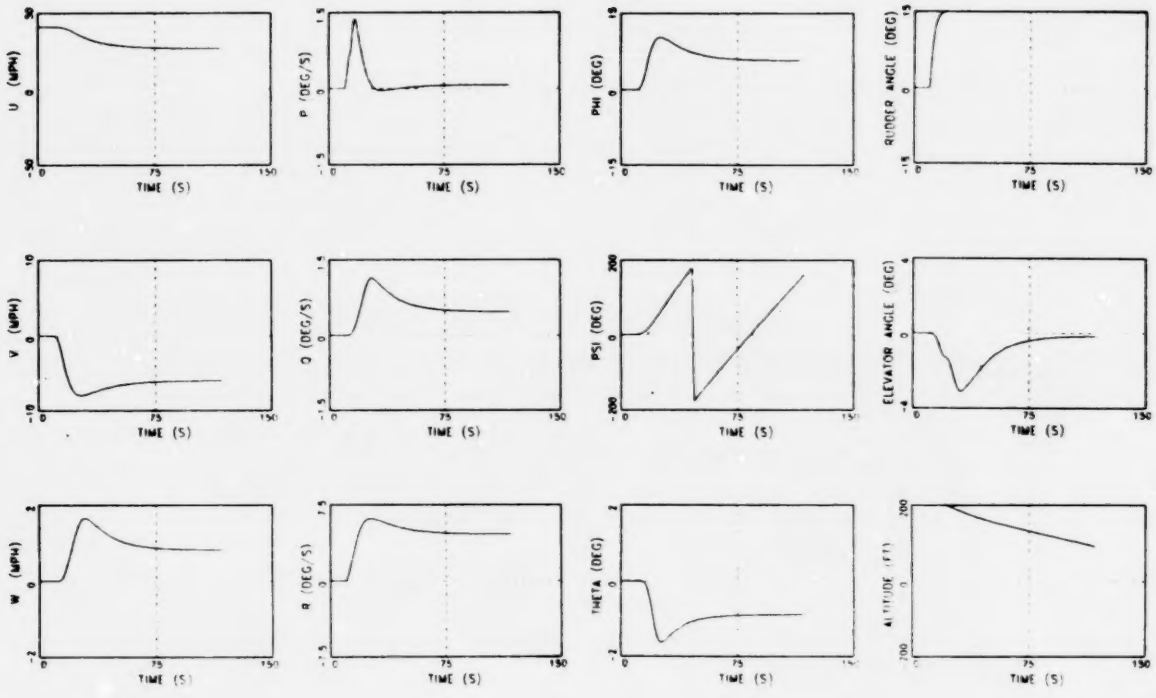

Fig 3 - Transient Response to Rudder Step

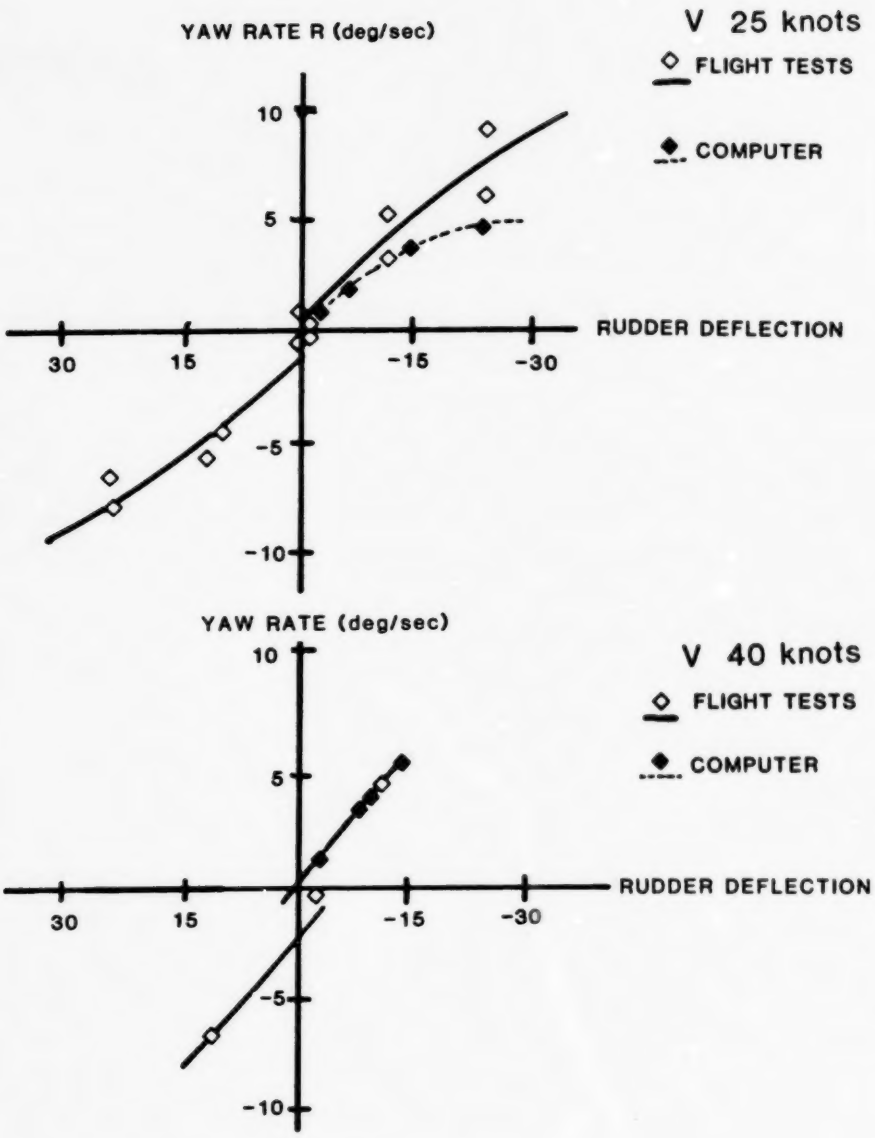

Fig 4 - Steady Yaw Rate vs Rudder Deflection

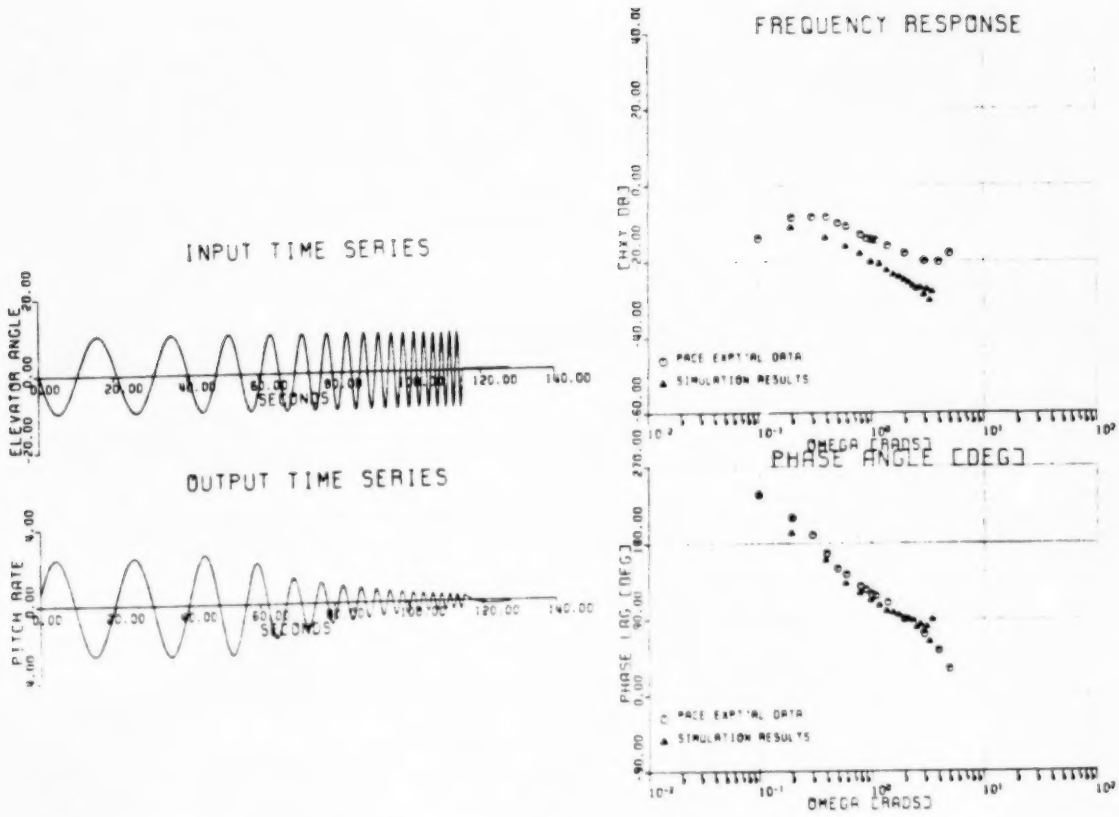

Fig 5 - Frequency Response of Pitch Rate to Elevator Input at 40 knots

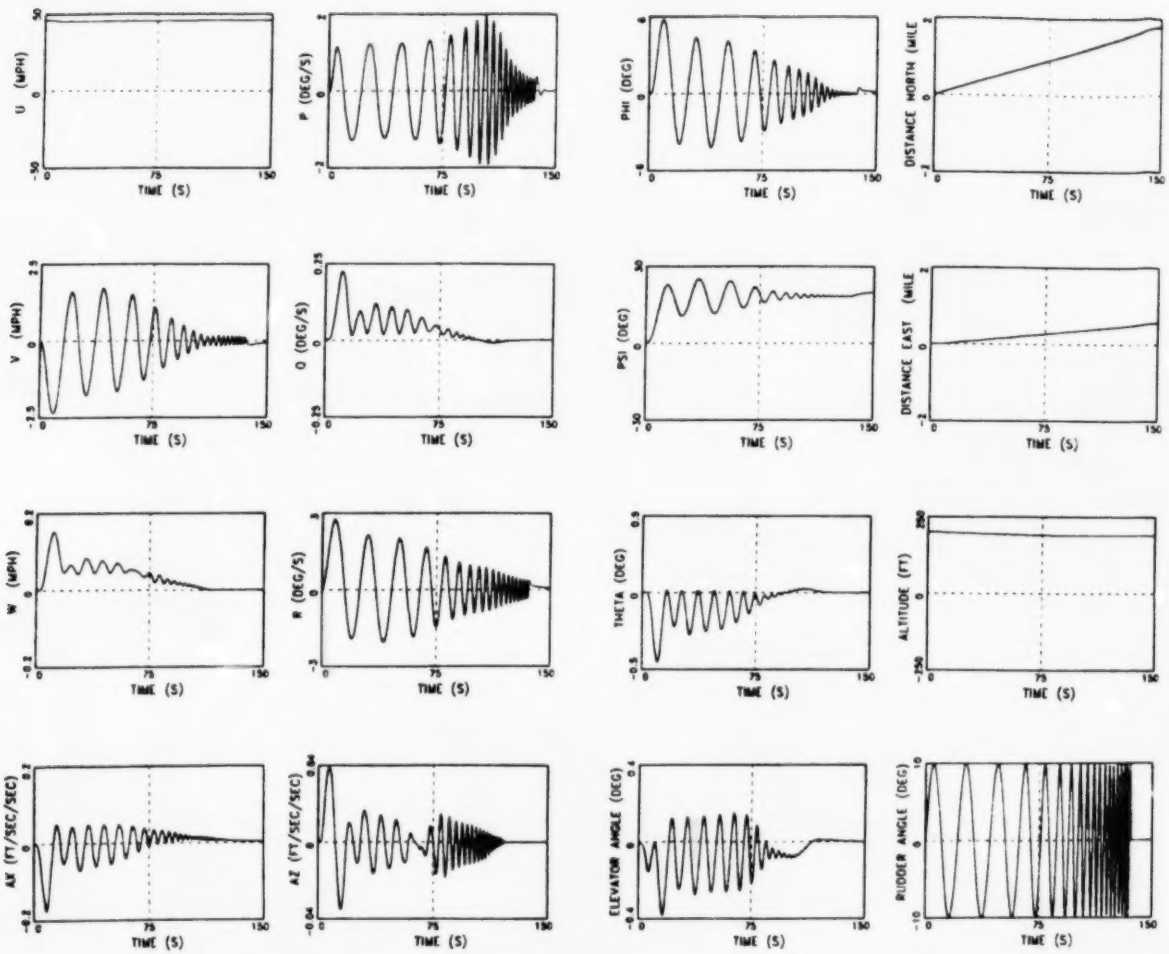

Fig 6 - Predicted Response of Skyship 500 to Rudder Sweep at 40 knots

Fig.7 Frequency Response of Roll Rate to Rudder Input

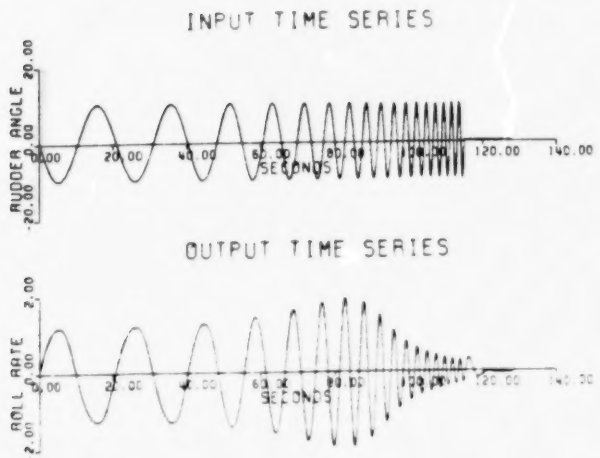

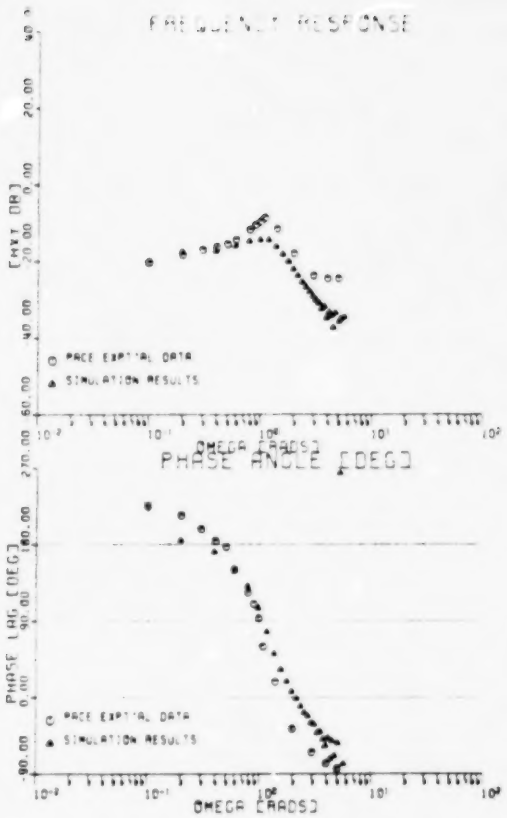

Fig.8 Frequency Response of Yaw Rate to Rudder Input

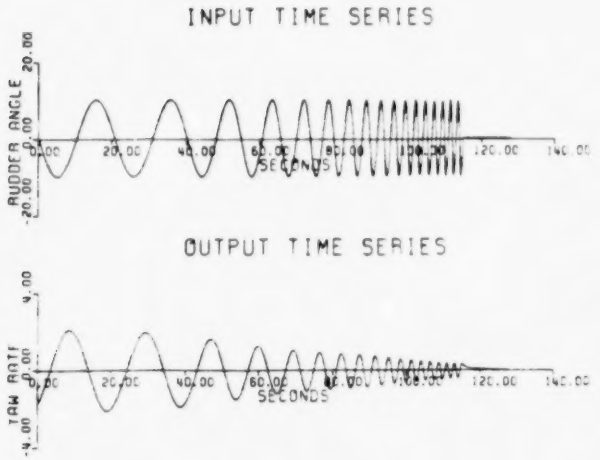

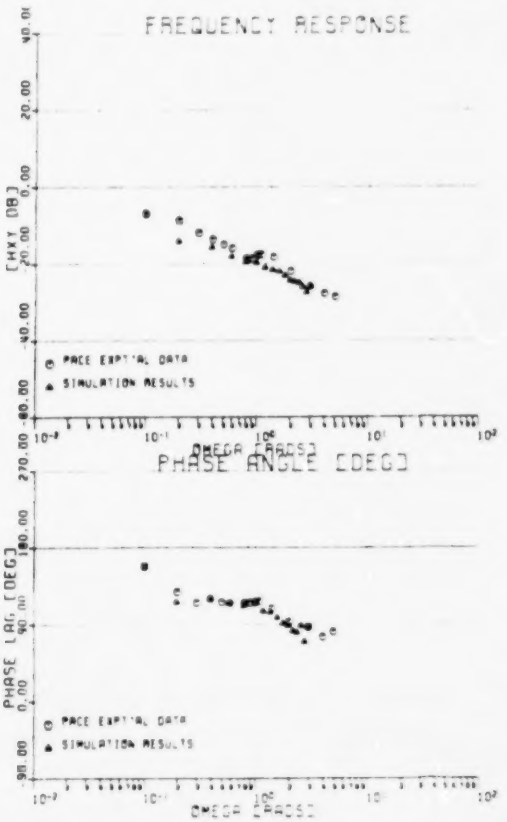

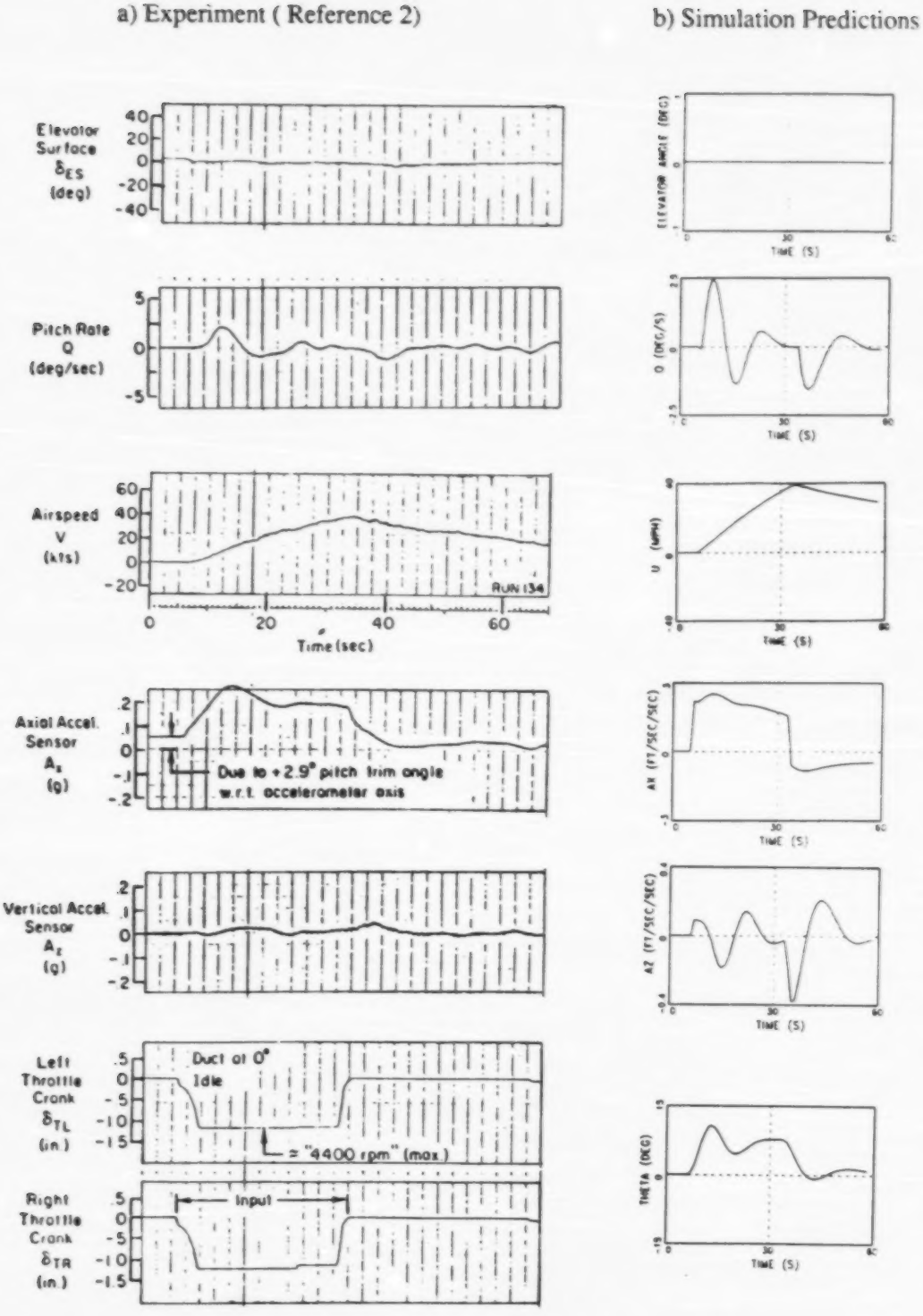

Fig.9 Response to Throttle Step and Return From Hover - Forward Thrust

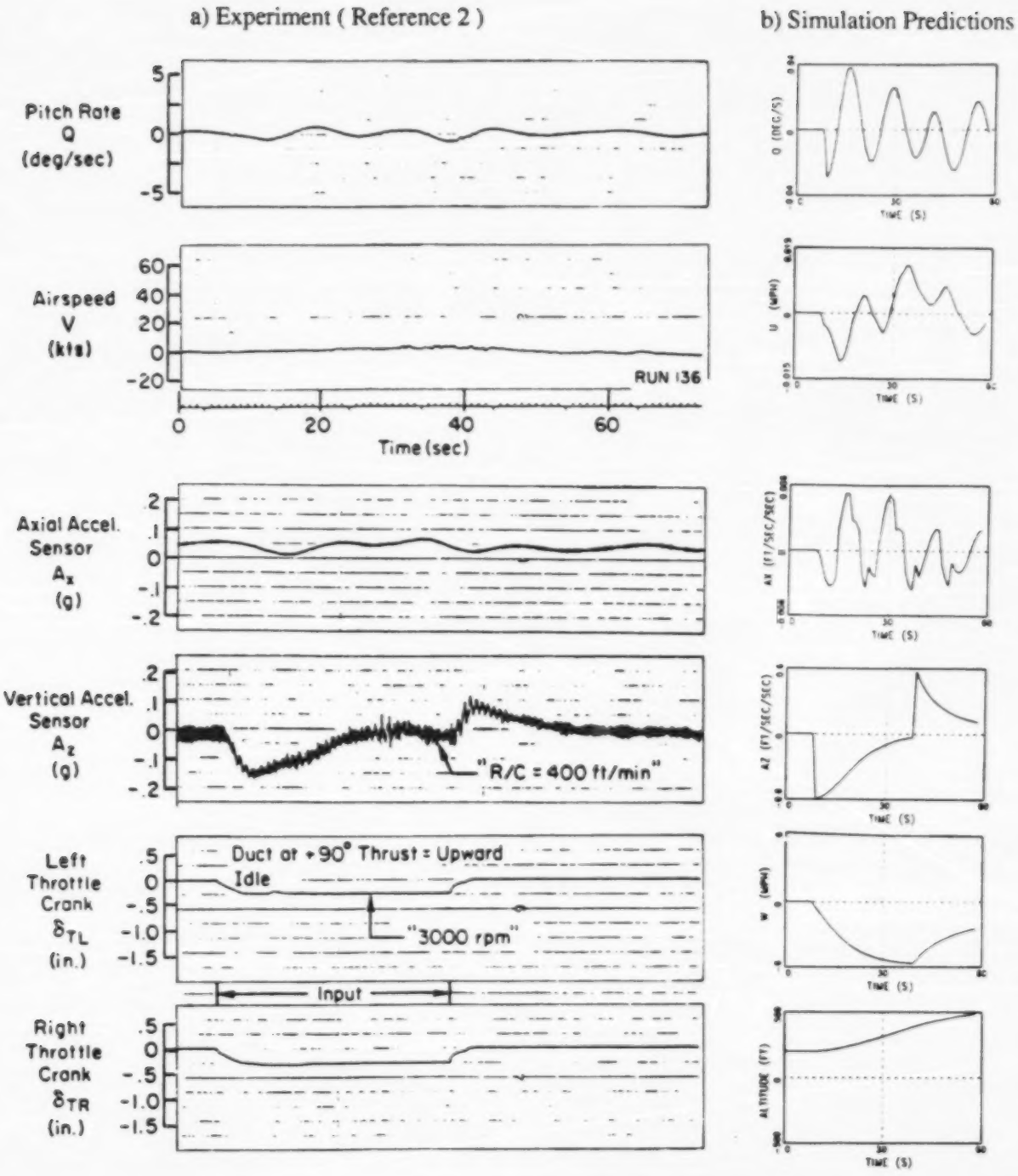

Fig.10 Response to Throttle Step and Return From Hover - Upward Thrust

a) Experiment (Reference 2)

b) Simulation Predictions

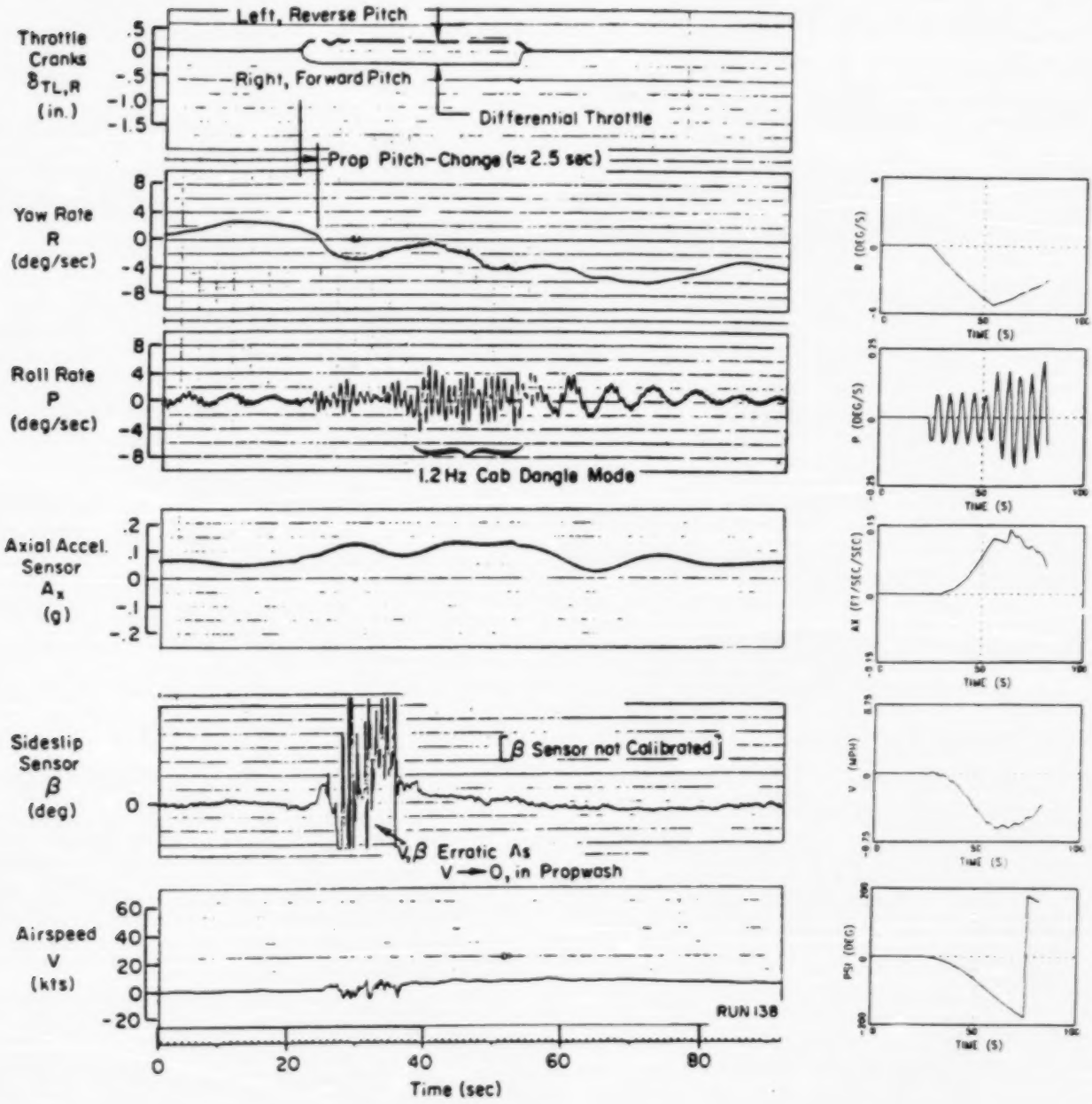

Fig.11 Response to Throttle Step and Return From Hover - Differential Thrust

TABLE 1

Summary of Basic SKYSHIP 500 Properties

Hull volume	=	181,200 ft^3 (5131 m^3)
Hull fineness ratio	=	3.57
Maximum hull diameter	=	45.93 ft (14.0 m)
Maximum hull length	=	164.04 ft (50.0 m)
Maximum takeoff weight	=	359.47 slugs (5250 kg)
Maximum cruise speed	=	55 knots (115 km/h)

TABLE 2

Summary of Estimated SKYSHIP 500 Properties

Hull equation: $R = (Ax + Bx^2 + Cx^3 + Dx^4)^{1/2}$

R = hull radius in feet

x = axial distance from the nose in feet

A = 15.16689974

B = -0.12708906

C = 2.3974271×10^{-4}

D = $-1.7454597 \times 10^{-7}$

Fin weight:	273.2 lb/fin	(124.2 kg)
Nose cone with battens:	242.0 lb	(110.0 kg)
Nose ballast:	165.0 lb	(75.0 kg)
Envelope weight:	2638.0 lb	(1199 kg)
Gondola weight:	3865.0 lb	(1756.8 kg)
Manufacturer's weight empty:	248.62 slugs	(3639 kg)

Payload weight :	0 % ballonet	3570 lb	(1622.7 kg)
	12 % ballonet	2305 lb	(1047.7 kg)
	26 % ballonet	663 lb	(301.4 kg)

TABLE 3

Hull Physical Properties (Ballonet Volume = 12% Hull Volume)

Buoyancy Ratio = 1

Section No.	Air Volume		Helium Volume	
	(ft^3)	(m^3)	(ft^3)	(m^3)
1	0.	0.	5563.	157.53
2	4507.	127.63	12400.	351.14
3	4507.	127.63	19904.	563.64
4	0.	0.	28317.	801.88
5	0.	0.	29027.	821.98
6	0.	0.	26920.	762.32
7	4507.	127.63	12667.	358.70
8	4507.	127.63	19191.	543.45
9	0.	0.	4557.	129.04

Section No.	Air Centre of Volume				Helium Centre of Volume			
	X		Z		X		Z	
	(ft)	(m)	(ft)	(m)	(ft)	(m)	(ft)	(m)
1	0.	0.	0.	0.	11.	3.35	0.	0.
2	29.	8.84	6.53	1.99	25.	7.62	-2.374	-0.724
3	39.	11.89	6.53	1.99	45.	13.72	-1.479	-0.451
4	0.	0.	0.	0.	61.	18.59	0.	0.
5	0.	0.	0.	0.	79.	24.08	0.	0.
6	0.	0.	0.	0.	97.	29.57	0.	0.
7	115.	35.05	6.38	1.94	112.	34.14	-2.268	-0.691
8	124.	37.80	6.38	1.94	133.	40.54	-1.497	-0.456
9	0.	0.	0.	0.	152.	46.33	0.	0.

Total Air Volume = 18028.1 ft^3 (510.5 m^3)
Total Helium Volume = 158546.3 ft^3 (4,490.0 m^3)

TABLE 3 cont'd

Section No.	Axial Centre of Mass		Vertical Centre of Mass	
	Xcg(1)		Zcg(1)	
	(ft)	(m)	(ft)	(m)
1	9.9	3.0	0.0	0.0
2	27.1	8.3	2.5	0.76
3	41.9	12.8	2.1	0.64
4	61.1	18.6	0.0	0.0
5	72.7	22.2	23.8	7.25
6	96.8	29.5	0.0	0.0
7	113.3	34.5	2.5	0.76
8	129.6	39.5	1.9	0.58
9	153.2	46.7	0.0	0.0

Section No.	Segment Weight		Buoyancy	
	(lb)	(kg)	(lb)	(kg)
1	210.	95.5	426.	193.6
2	773.	351.4	1294.	588.2
3	920.	418.2	1868.	849.1
4	701.	318.6	2167.	985.
5	6884.	3129.1	2222.	1010.
6	675.	306.8	2060.	936.4
7	740.	336.4	1314.	597.3
8	983.	446.8	1814.	824.5
9	186.	84.5	349.	158.6

X location centre of mass = 77.8 ft (23.7 m)
Z location centre of mass = 12.8 ft (3.90 m)
X location centre of buoyancy = 78.9 ft (24.05 m)
Total weight = 13514 lb (6143 kg)

TABLE 3 cont'd

Section moments of inertia are referenced to the local section centre of gravity.

Section No.	Ixx (slug-ft^2)	Iyy (slug-ft^2)	Izz (slug-ft^2)	Ixz (slug-ft^2)
1	6.691e+02	4.513e+03	4.513e+03	0.
2	3.087e+03	1.996e+03	1.684e+03	-2.397e+02
3	4.947e+03	3.047e+03	2.729e+03	4.115e+02
4	5.679e+03	3.145e+03	3.145e+03	0.
5	2.647e+04	1.828e+04	4.208e+03	2.927e+04
6	5.274e+03	2.936e+03	2.936e+03	0.
7	3.477e+03	2.003e+03	1.712e+03	6.877e+03
8	4.021e+03	3.337e+03	3.027e+03	2.230e+04
9	4.553e+02	3.699e+02	3.699e+02	0.

Total vehicle moments of inertia are referenced to the vehicle's centre of mass.

Ixx(total) = 122,700 slug-ft^2 (354.1 kg-m^2)
Iyy(total) = 573400 slug-ft^2 (1,654.9 kg-m^2)
Izz(total) = 505,000 slug-ft^2 (1,457.5 kg-m^2)
Ixz(total) = 82,530 slug-ft^2 (238.2 kg-m^2)

TABLE 4

List of Aerodynamic Parameters

Parameter	Value
$(C_{dc})_f$	2.11
$(C_{dc})_h$	0.200
$(C_{df})_o$	0.0050
$(C_{dh})_o$	0.0045
$(C_{n\alpha})_f$	2.63
a_2	0.618
c	23.03 ft (7.02 m)
k_1	0.0988
k_2 , k_3	0.8361
$(k_3 - k_1)$	0.7373
M_{a1}	42.55 slugs (622 kg)
M_{a2} , M_{a3}	360.10 slugs (5264 kg)
η_f	0.700
η_k	1.13
η_t	0.94
J_1	5827 ft^2 (541 m^2)
S_{fe}	290.1 ft^2 (27.0 m^2)
S_f	1462.8 ft^2 (135.9 m^2)

APPENDIX I : System Equations of Motion

The coefficients of the system inertia matrix are given by the following set of equations:[7]

$$A_{11} = m \tag{II-1}$$

$$A_{15} = m z_{cg} \tag{II-2}$$

$$A_{16} = -m y_{cg} \tag{II-3}$$

$$A_{22} = m \tag{II-4}$$

$$A_{24} = -m z_{cg} \tag{II-5}$$

$$A_{26} = m x_{cg} \tag{II-6}$$

$$A_{33} = m \tag{II-7}$$

$$A_{34} = m y_{cg} \tag{II-8}$$

$$A_{35} = -m x_{cg} \tag{II-9}$$

$$A_{42} = -m z_{cg} \tag{II-10}$$

$$A_{43} = m y_{cg} \tag{II-11}$$

$$A_{44} = I_{xx} + m\left(z_{cg}^2 + y_{cg}^2\right) \tag{II-12}$$

$$A_{45} = -m x_{cg} y_{cg} \tag{II-13}$$

$$A_{46} = -I_{xz} - m x_{cg} z_{cg} \tag{II-14}$$

$$A_{51} = m z_{cg} \tag{II-15}$$

$$A_{53} = -m x_{cg} \tag{II-16}$$

$$A_{54} = -m x_{cg} y_{cg} \tag{II-17}$$

$$A_{55} = I_{yy} + m\left(x_{cg}^2 + z_{cg}^2\right) \tag{II-18}$$

$$A_{56} = -m y_{cg} z_{cg} \tag{II-19}$$

$$A_{61} = -mY_{cg} \tag{II-20}$$

$$A_{62} = mX_{cg} \tag{II-21}$$

$$A_{64} = -I_{xz} - mX_{cg}\bar{z}_{cg} \tag{II-22}$$

$$A_{65} = -mY_{cg}\bar{z}_{cg} \tag{II-23}$$

$$A_{66} = I_{zz} + m(X_{cg}^2 + Y_{cg}^2) \tag{II-24}$$

Equation (2.1) in expanded form is given by the following set of equations:[7]

$$A_{11}\dot{U} + A_{15}\dot{Q} + A_{16}\dot{R} = F_X \tag{II-25}$$

$$\begin{aligned} F_X &= F_X^A + R(A_{22}V + A_{24}P + A_{26}R) \\ &\quad - Q(A_{33}W + A_{34}P + A_{35}Q) \\ &= F_X^A + F_X^V \end{aligned} \tag{II-26}$$

$$A_{22}\dot{V} + A_{24}\dot{P} + A_{26}\dot{R} = F_Y \tag{II-27}$$

$$\begin{aligned} F_Y &= F_Y^A + P(A_{33}W + A_{34}P + A_{35}Q) \\ &\quad - R(A_{11}U + A_{15}Q + A_{16}R) \\ &= F_Y^A + F_Y^V \end{aligned} \tag{II-28}$$

$$A_{33}\dot{W} + A_{34}\dot{P} + A_{35}\dot{Q} = F_Z \tag{II-29}$$

$$\begin{aligned} F_Z &= F_Z^A + Q(A_{11}U + A_{15}Q + A_{16}R) \\ &\quad - P(A_{22}V + A_{24}P + A_{26}R) \\ &= F_Z^A + F_Z^V \end{aligned} \tag{II-30}$$

$$A_{44}\dot{P} + A_{24}\dot{V} + A_{34}\dot{W} + A_{45}\dot{Q} + A_{46}\dot{R} = L \tag{II-31}$$

$$\begin{aligned} L &= L^A + W(A_{22}V + A_{24}P + A_{26}R) \\ &\quad - V(A_{33}W + A_{34}P + A_{35}Q) \\ &\quad + R(A_{55}Q + A_{15}V + A_{35}W + A_{45}P + A_{56}R) \\ &\quad - Q(A_{66}R + A_{16}U + A_{26}V + A_{46}P + A_{56}Q) \\ &= L^A + L^V \end{aligned} \tag{II-32}$$

$$A_{55}\dot{Q} + A_{15}\dot{U} + A_{35}\dot{W} + A_{45}\dot{P} + A_{56}\dot{R} = M \qquad \text{(II-33)}$$

$$\begin{aligned} M = M^A &+ U(A_{33}W + A_{34}P + A_{35}Q) \\ &- W(A_{11}U + A_{15}Q + A_{16}R) \\ &+ P(A_{66}R + A_{16}U + A_{26}V + A_{46}P + A_{56}Q) \\ &- R(A_{44}P + A_{24}V + A_{34}W + A_{45}Q + A_{46}R) \\ &= M^A + M^V \end{aligned} \qquad \text{(II-34)}$$

$$A_{66}\dot{R} + A_{16}\dot{U} + A_{26}\dot{V} + A_{46}\dot{P} + A_{56}\dot{Q} = N \qquad \text{(II-35)}$$

$$\begin{aligned} N = N^A &+ V(A_{11}U + A_{15}Q + A_{16}R) \\ &- U(A_{22}V + A_{24}P + A_{26}R) \\ &+ Q(A_{44}P + A_{24}V + A_{34}W + A_{45}Q + A_{46}R) \\ &- P(A_{55}Q + A_{15}U + A_{35}W + A_{45}P + A_{57}R) \\ &= N^A + N^V \end{aligned} \qquad \text{(II-36)}$$

Note that the lateral offset of the centre of gravity, Y_{cg}, is usually zero